Ge-on-Si laser operating at room temperature

Jifeng Liu,* Xiaochen Sun, Rodolfo Camacho-Aguilera, Lionel C. Kimerling, and Jurgen Michel

MIT Microphotonics Center, Department of Materials Science and Engineering, Massachusetts Institute of Technology, Cambridge, Massachusetts 02139, USA
Corresponding author: jfliu01@mit.edu

Monolithic lasers on Si are ideal for high-volume and large-scale electronic–photonic integration. Ge is an interesting candidate owing to its pseudodirect gap properties and compatibility with Si complementary metal oxide semiconductor technology. Recently we have demonstrated room-temperature photoluminescence, electroluminescence, and optical gain from the *direct* gap transition of band-engineered Ge-on-Si using tensile strain and *n*-type doping. Here we report what we believe to be the first experimental observation of lasing from the *direct* gap transition of Ge-on-Si at room temperature using an edge-emitting waveguide device. The emission exhibited a gain spectrum of 1590–1610 nm, line narrowing and polarization evolution from a mixed TE/TM to predominantly TE with increasing gain, and a clear threshold behavior. © 2010 Optical Society of America

OCIS codes: 130.5990, 160.3380, 250.5960.

Monolithically integrated lasers on Si have long been one of the biggest challenges for Si-based electronic–photonic integration [1]. Previous investigations include Si and SiGe nanostructures [2–4], Er doped Si-based materials [5,6], GeSn [7,8], β-FeSi$_2$ [9], and hybrid III–V lasers on Si [10,11]. Recently, our theoretical analysis has shown that Ge, traditionally considered an indirect gap material, can be band engineered to behave like a direct-gap material by using tensile strain and *n*-type doping to compensate the energy difference between the direct and indirect conduction valleys [12]. Indeed, direct gap photoluminescence (PL) [13,14], electroluminescence (EL) [15], and optical gain [16] at room temperature have been demonstrated in tensile-strained n^+ Ge-on-Si. Here we report the first (to our knowledge) observation of lasing from the direct-gap transition of Ge-on-Si at room temperature using an edge-emitting waveguide device. The emission exhibited a gain spectrum in the wavelength range of 1590–1610 nm, line narrowing and polarization evolution from a mixed TE/TM to predominantly TE with increasing gain, and a clear threshold behavior.

The device used in the experimental study of lasing from tensile strained n^+ Ge consists of trench-grown multimode Ge waveguides with mirror-polished facets monolithically integrated on an Si wafer. The Ge waveguides were selectively grown epitaxially on Si by ultrahigh vacuum chemical vapor deposition using an SiO$_2$ mask layer. Details about the selective growth were reported earlier [17]. The Ge material was fully relaxed at the growth temperature of 650°C, and 0.24% thermally induced tensile strain was accumulated upon cooling to room temperature. The tensile strain shrinks the direct gap of Ge to 0.76 eV so that its difference from the indirect gap is reduced. The Ge material was *in situ* doped with 1 $\times 10^{19}$ cm^{-3} phosphorous during the growth to further compensate the energy difference between the direct (Γ) and indirect (L) conduction valleys and significantly enhance the direct gap light emission [13,14,16]. A cross-sectional scanning electron microscopy (SEM) picture of the Ge waveguide is shown in the inset of Fig. 1. The width of the Ge waveguide is 1.6 μm, and the height is 500 nm. The relatively large cross-sectional dimensions were selected conservatively to guarantee >90% optical confinement in the Ge gain medium for demonstration of lasing, without optimization for the minimal threshold. The edges of the samples were mirror polished to obtain vertical facets for reflection mirrors on both ends of the waveguides. The length of the waveguides is 4.8 mm. Such a long waveguide was chosen to guarantee a mirror loss of ≪10 cm^{-1}, which is much smaller than the optical gain of Ge [16]. The reflectivity at an ideal facet is estimated to be 37%, considering the index contrast between Ge and air, corresponding to a mirror loss of 2 cm^{-1}.
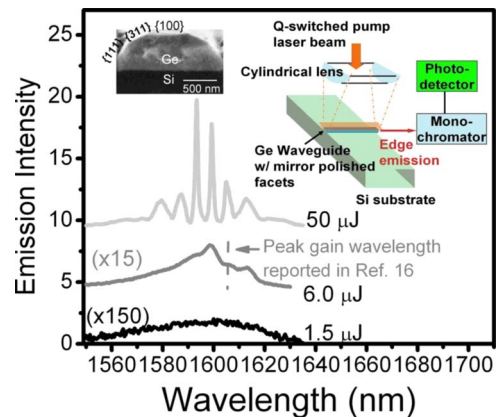

Fig. 1. (Color online) Edge-emission spectra of a Ge waveguide with mirror polished facets under 1064 nm excitation from a *Q*-switched laser with a pulse duration of 1.5 ns and a repetition rate of 1 kHz. The spectral resolution of the measurement was 2 nm. The three spectra at 1.5, 6.0, and 50 μJ/pulse pumping power correspond to spontaneous emission, threshold for lasing, and laser emission. The arrow indicates the peak optical gain wavelength reported in [16]. The inset shows a cross-sectional SEM picture of the Ge waveguide and a schematic drawing of the experimental setup for optical pumping.

The experimental setup for optical pumping is schematically shown in the inset of Fig. 1. The entire waveguide was excited by a 1064 nm Q-switched laser with a pulse duration of 1.5 ns and a maximum output of 50 μJ/pulse operating at a repetition rate of 1 kHz. The pump laser was focused into a line of $\sim$7 mm long and $\sim$0.5 mm wide by a cylindrical lens and vertically incident on top of a Ge waveguide, as schematically shown in the inset of Fig. 1. Considering $\sim$10% coupling losses due to lenses and mirrors in the system, $\sim$37% reflection loss at the Ge surface, and an absorbance of $\sim$0.6 for 500-nm-thick Ge at 1064 nm using an absorption coefficient of 16000 cm^{-1} reported in [18], the actual peak pump power density absorbed by Ge is $\sim$300 kW/cm^2 for 50 μ J/pulse output power. The pulsed edge emission from the Ge waveguides is collected into a monochromator and detected by an InGaAs photomultiplier.

Figure 1 shows the light emission spectra of a Ge waveguide under different pumping levels with a spectral resolution of 2 nm. At 1.5 μJ/pulse, the emission from the waveguide shows a broad band with a maximum around 1600 nm, consistent with PL and EL spectra of 0.2% tensile strained Ge reported earlier [13–15]. Clearly, at this stage spontaneous emission dominates the spectrum. As the pump power increases to 6.0 μJ/pulse, emission peaks emerge at 1599, 1606, and 1612 nm, and a shoulder appears at 1594 nm. This change in the emission spectrum occurs at the pump power corresponding to the threshold behavior in Fig. 2, marking the onset of transparency from −100 cm^{-1} loss to $\sim$50 cm^{-1} gain [16]. The emergence of emission peaks between 1600 and 1610 nm at the threshold of lasing is also remarkably consistent with the optical-gain spectrum peaked at 1605 nm reported in [16]. As pump power increases to 50 μJ/pulse, the widths of the emission peaks at 1594, 1599, and 1605 nm significantly decrease, while the polarization evolved from a mixed TE/TM to predominantly TE with a contrast ratio of 10:1 owing to the increase of optical gain, as expected for typical lasing behavior. The strongest emission peak blueshifts from 1600 nm to 1594 nm, and two new

peaks appear at shorter wavelengths. This result is consistent with the fact that the gain spectrum shifts to shorter wavelengths with the increase of carrier injection due to occupation of higher energy states in the direct Γ valley [12]. The two strongest and narrowest emission lines at 1593.6 and 1599.2 nm are most likely due to higher gain coefficients compared to other wavelengths. This explanation is also consistent with typical bell shapes of gain spectra, where maximum material gain is achieved at photon energies slightly larger than the band gap ($\sim$17 meV above the band gap in this case). The multiple emission peaks are most likely due to multiple guided modes in the Ge waveguide. In fact, nine guided modes are supported in the Ge waveguides used in this study because of the high index contrast between Ge (4.2) and air (1.0). The effective refractive indexes of the first six modes are very close, ranging from 4.08 to 3.82. Coexistence of lasing modes can be enabled by a broad-enough gain spectrum under a high excitation of 300 kW/cm^2 in this case. Indeed, similar behavior has been observed in an early work on multimode III–V semiconductor lasers, where two modes of comparable emission intensity were observed in the spectrum with a separation of 10 nm [19].

Figure 2 shows the integral emission intensity versus pump power. An obvious threshold behavior is demonstrated. The threshold pumping energy is $\sim$5μJ, consistent with the emission spectrum in Fig. 1 under 6 μJ optical pumping that shows the emergence of emission peaks between 1600 and 1610 nm. The absorbed pump power density at threshold is $\sim$30 kW/cm^2, corresponding to $\sim$35 kA/cm^2 injection current density in electrical pumping. The threshold current density is expected to decrease to several kA/cm^2 with increased n-type doping concentration in Ge [12]. The n-type doping level of low 10^{19} cm^{-3} in this study is limited by the out-diffusion of phosphorous during the Ge growth and can be improved by process optimization considering that the solubility of P in Ge is larger than 10^{20} cm^{-3} [20].

Figure 3 shows a high resolution scan of the emission line at 1593.6 nm using the highest available
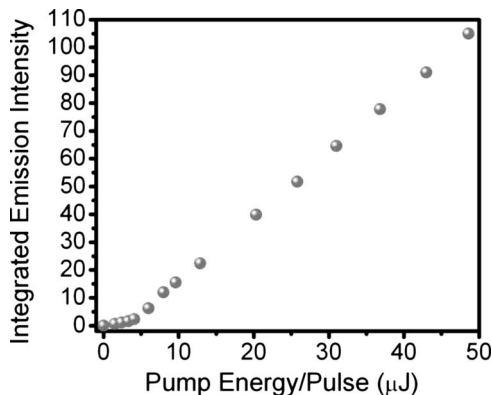

Fig. 2.   Integral emission intensity from the waveguide facet versus optical pump power showing the lasing threshold. The pump pulse width is 1.5 ns, and the absorbed pump power density at threshold is 30 kW/cm^2. The spectral resolution of the measurement was 2 nm.
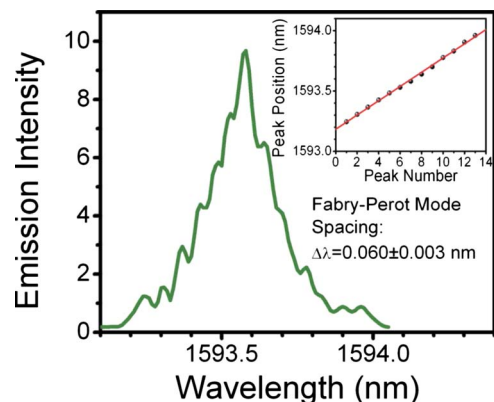

Fig. 3.   (Color online) High-resolution scan of the emission line at 1593.6 nm using the highest available spectral resolution of 0.1 nm. Longitudinal Fabry–Perot modes are clearly observed, and the period is consistent with the Ge waveguide cavity length of 4.8 mm.

resolution of the measurement system of 0.1 nm. Periodic peaks corresponding to longitudinal Fabry–Perot modes are clearly observed in the spectrum, similar to early reports on III–V semiconductor lasers with Fabry–Perot cavities under short pulse optical pumping [21,22]. The linear fit shown in the inset of Fig. 3 indicates a longitudinal mode spacing of 0.060 ± 0.003 nm, in good agreement with the calculated Fabry–Perot mode spacing of 0.063 nm for a 4.8-mm-long Ge waveguide cavity. The incomplete separation of the longitudinal modes is typical of short pulse pumping owing to transient changes in gain spectrum and refractive index [20,21], convolved with the resolution limit of the system in this case.

In conclusion, we have demonstrated an optically pumped edge-emitting multimode Ge-on-Si laser operating at room temperature with a gain spectrum of $1590-1610$ nm. Evidence of lasing consists of line narrowing and polarization evolution from a mixed TE/TM to predominantly TE with increasing gain, and a clear threshold behavior marking the onset of transparency. The gain spectrum is remarkably consistent with the band structure of tensile strained Ge observed previously [16]. Considering that Ge has already been applied to Si CMOS electronics and integrated photonic devices, a Ge-on-Si laser is a desirable choice for monolithic electronic–photonic integrated circuits.

References

1. D. J. Lockwood and L. Pavesi, in *Silicon Photonics* (Springer-Verlag, 2004), pp. 1–50.
2. N. Koshida and H. Koyama, Appl. Phys. Lett. **60**, 347 (1992).
3. L. Pavesi, L. Dal Negro, C. Mazzoleni, G. Franzo, and F. Priolo, Nature **408**, 440 (2000).
4. C. S. Peng, Q. Huang, W. Q. Cheng, J. M. Zhou, Y. H. Zhang, T. T. Sheng, and C. H. Tung, Phys. Rev. B **57**, 8805 (1998).
5. B. Zheng, J. Michel, F. Y. G. Ren, L. C. Kimerling, D. C. Jacobson, and J. M. Poate, Appl. Phys. Lett. **64**, 2842 (1994).
6. A. J. Kenyon, P. F. Trwoga, M. Federighi, and C. W. Pitt, J. Phys. Condens. Matter **6**, L319 (1994).
7. R. A. Soref and L. Friedman, Superlattices Microstruct. **14**, 18 (1993).
8. G. He and H. A. Atwater, Phys. Rev. Lett. **79**, 1937 (1997).
9. D. Leong, J. Harry, K. J. Reeson, and K. P. Homewood, Nature **387**, 686 (1997).
10. M. E. Groenert, C. W. Leitz, A. J. Pitera, V. Yang, H. Lee, R. J. Ram, and E. A. Fitzgerald, J. Appl. Phys. **93**, 362 (2003).
11. A. W. Fang, H. Park, O. Cohen, R. Jones, M. J. Paniccia, and J. E. Bowers, Opt. Express **14**, 9203 (2006).
12. J. Liu, X. Sun, D. Pan, X. X. Wang, L. C. Kimerling, T. L. Koch, and J. Michel, Opt. Express **15**, 11272 (2007).
13. J. F. Liu, X. C. Sun, P. Becla, L. C. Kimerling, and J. Michel, in *5th IEEE International Conference on Group IV Photonic* (2008), pp. 16–18.
14. X. C. Sun, J. F. Liu, L. C. Kimerling, and J. Michel, Appl. Phys. Lett. **95**, 011911 (2009).
15. X. C. Sun, J. F. Liu, L. C. Kimerling, and J. Michel, Opt. Lett. **34**, 1198 (2009).
16. J. F. Liu, X. C. Sun, L. C. Kimerling, and J. Michel, Opt. Lett. **34**, 1738 (2009).
17. H. Luan, D. R. Lim, K. K. Lee, K. M. Chen, J. G. Sandland, K. Wada, and L. C. Kimerling, Appl. Phys. Lett. **75**, 2909 (1999).
18. M. V. Hobalen, J. Phys. Chem. Solids **23**, 821 (1962).
19. R. C. Miller, W. A. Nordland, R. A. Logan, and L. F. Johnson, J. Appl. Phys. **49**, 539 (1977).
20. *Physics of Group IV Elements and III–V Compounds*, O. Madelung, ed. (Springer, Berlin, 1982), Vol. 22b, p. 448.
21. D. Botez, L. Figueroa, and S. Wang, Appl. Phys. Lett. **29**, 502 (1976).
22. F. A. Blum, K. L. Lawley, W. C. Scott, and W. C. Holton, Appl. Phys. Lett. **24**, 430 (1974).